MobileIPL: Enhancing Mobile Agents Thinking Process via Iterative Preference Learning

Anonymous authors
Paper under double-blind review

Abstract

The Chain of Action-Planning Thoughts (CoaT) paradigm has been shown to improve the reasoning performance of VLM-based mobile agents in GUI tasks. However, the scarcity of diverse CoaT trajectories limits the expressiveness and generalization ability of such agents. While self-training is commonly employed to address data scarcity, existing approaches either overlook the correctness of intermediate reasoning steps or depend on expensive process-level annotations to construct process reward models (PRM). To address the above problems, we propose an **I**terative **P**reference **L**earning (*IPL*) that constructs a CoaT-tree through interative sampling, scores leaf nodes using rule-based reward, and backpropagates feedback to derive Thinking-level Direct Preference Optimization (T-DPO) pairs. To prevent overfitting during warm-up supervised fine-tuning, we further introduce a three-stage instruction evolution, which leverages GPT-4o to generate diverse Q&A pairs based on real mobile UI screenshots, enhancing both generality and layout understanding. Experiments on three standard Mobile GUI-agent benchmarks demonstrate that our agent *MobileIPL* outperforms strong baselines, including continual pretraining models such as OS-ATLAS and UI-TARS. It achieves state-of-the-art performance across three standard Mobile GUI-Agents benchmarks and shows strong generalization to out-of-domain scenarios.

1 Introduction

VLM-based mobile agents (Wang et al., 2023; Ding, 2024) have attracted considerable attention due to their ability to seamlessly interact with mobile graphical user interfaces (GUIs) and their potential to autonomously perform daily tasks. Since actions are not directly specified in user instructions, mobile agents benefit from generating intermediate thoughts aligned with the current GUI context. Recent work such as AITZ(Zhang et al., 2024b) has demonstrated that the Chain of Action-Planning Thoughts (CoaT) pattern—resembling the slow-thinking "System 2" process—is particularly effective in GUI domains.

However, directly applying supervised fine-tuning (SFT) on CoaT trajectories may cause overfitting, leading the model to be trapped in fixed reasoning patterns. To address this limitation, recent studies in the general domain have explored self-training strategies. These approaches typically utilize the correctness of the final answer in output as a reward signal to train the model(Luong et al., 2024). While effective in some contexts, relying solely on final answers overlooks the quality of intermediate reasoning steps, which can result in reward hacking and suboptimal reasoning processes. Some search-based approaches, such as ReST-MCTS (Xie et al., 2024), tackle this problem by learning a process reward model (PRM) to evaluate individual reasoning steps. However, these approaches often require large-scale manual annotation of intermediate steps (Guo et al., 2025a). This challenge is especially severe in the Mobile GUI Agent domain. Unlike text-based tasks in coding or math, GUI environments rely on real devices or simulators, making step-level reward annotation significantly more costly and labor-intensive.

To address these limitations, we propose an iterative sampling framework that constructs a CoaT-tree based on Monte Carlo Tree Search (MCTS). Instead of relying on a PRM, we score each reasoning step and construct thinking-level DPO (T-DPO) pairs without manual step annotation. Specifically, we perform multi-turn dialogue with a vision-language model (VLM) to incrementally build a CoaT-tree, where each node corresponds to a sampled response at a given reasoning step, conditioned on the dialogue history. This hierarchical structure captures diverse reasoning paths and facilitates fine-grained assessment of intermediate thoughts. We first assign rewards to the leaf node, and then propagate these signals backward through the CoaT-tree to earlier reasoning steps. Based on the resulting values, we construct thinking-level DPO pairs to help agents optimize both final actions and the overall quality of their reasoning.

To mitigate the lack of diversity after warm-up SFT, we adopt an instruction evolution strategy. Specifically, we generate diverse Q&A pairs grounded in real mobile UI screenshots from downstream training datasets. These Q&A pairs serve two purposes: (1) prevent agents from overfitting to static downstream instructions by introducing varied reasoning contexts, and (2) improve agents' understanding of UI layouts through visually grounded question-answering. We evaluate our approach on the CoaT dataset AITZ and long-horizon dataset AMEX, where it outperforms state-of-the-art GUI-agent continual pretraining agents such as OS-ATLAS (Wu et al., 2024) (+4.04%) and UI-TARS (Qin et al., 2025) (+3.54%). Furthermore, experiments on the AndroidControl dataset demonstrate the strong generalization capability of our method to unseen apps and instructions (tasks). Under limited training resources, IPL consistently outperforms naive DPO using only half of the data for one iterative training round (+4.5%), or one-fifth of the data for two iterative training rounds (+0.3%). Analytical experiments show instruction evolution simultaneously improves both the diversity and quality of reasoning.

Overall, our main contributions are summarized as follows:

•We propose an iterative framework to construct a CoaT-tree, and utilize rule-based rewards with backward credit assignment to form thinking-level DPO pairs for reasoning optimization.

• We introduce an instruction evolution strategy to mitigate overfitting during warm-up SFT, enhancing the model's generalization and UI understanding.

• We demonstrate the effectiveness of our method on three GUI-agent benchmarks: AITZ, AMEX, and AndroidControl. Furthermore, our approach even surpasses SoTA continual pretraining models.

2 Related Work

2.1 Mobile GUI Agent

LLMs (Achiam et al., 2023) are increasingly used as autonomous agents for mobile interaction (Li et al., 2024b; Wen et al., 2023). With the rapid development of vision-language models (VLMs), researchers build mobile GUI agents (Yang et al., 2023; Zheng et al., 2024; Qin et al., 2025; Team) and multi-agent frameworks (Ding, 2024; Li et al., 2024c; Wang et al., 2024a) based on closed-source VLMs. Meanwhile, some researchers focus on training agents with stronger element grounding (Cheng et al., 2024; Wu et al., 2024), page navigation (Niu et al., 2024; Lu et al., 2024; Gou et al., 2024; Wang et al., 2025), GUI understanding (You et al., 2024; Baechler et al., 2024) and task planning capabilities (Zhang et al., 2024c; Nong et al., 2024; Xu et al., 2024; Qinghong Lin et al., 2024; Dorka et al., 2024) based on open-source VLMs. Our method organizes trajectory data into multi-turns of dialogues based on the CoaT thinking pattern, preventing the agent becomes an action model with limited capabilities.

2.2 Reinforcement Learning

The algorithms applied in natural language processing to align with human preferences include Direct Preference Optimization (DPO) (Rafailov et al., 2023), Identity Preference Optimization (IPO) (Azar et al., 2024), Kahneman-Tversky Optimization (KTO) (Ethayarajh et al., 2023), and Proximal Policy Optimization (PPO) (Schulman et al., 2017). Specifically, ReFT (Luong et al., 2024) adopts reinforcement learning as a fine-tuning paradigm to improve performance on math problems. ReST-MCTS* (Zhang et al., 2024a) focuses on the higher-quality step reward, where the process reward model is important. Xie, et al. (Xie et al., 2024) label the preference via MCTS based on feedback from self-evaluation. For mobile GUI agents, Digirl (Bai et al., 2024) and Distrl (Wang et al., 2024c) use online trajectory collection to improve the generalization of agents whose process is very slow. Reachagent (Wu et al., 2025) uses DPO training to compare the quality of multiple actions. TCPO (Jiao et al., 2025) also optimizes thoughts, but does not explicitly enforce thought–action consistency. TreePO (Li et al., 2025), TreeRL (Hou et al., 2025), and SPO (Guo et al., 2025b) segment long sequences into many short segments, which leads to high computational cost and low data efficiency. In contrast, our method models thoughts with a fixed CoaT-tree and uses T-DPO to optimize the thinking process, while step values are computed directly from rule-based rewards, without unstable PRMs. This design yields more efficient sampling and training, especially in GUI-agent settings.

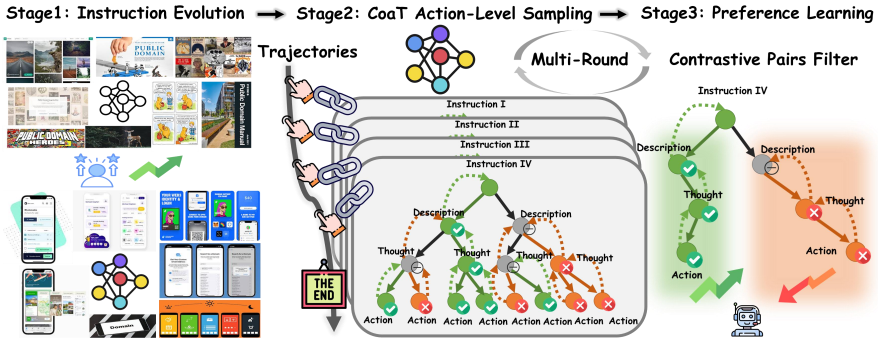

Figure 1: Overview of iterative preference learning framework. The left part presents the process of warm-up fine-tuning a general VLM to a mobile GUI domain agent with basic capabilities. The mid and right parts represent the iterative CoaT thinking-level sampling and T-DPO training process.

3 Methodology

In this section, we first introduce the multi-turn thinking process formulation (§ 3.1) and explain our method. As shown in Figure 1, our method starts with instruction evolution strategy (§ 3.2) to enhance output diversity in warm-up SFT stage. Then, a CoaT-tree through iterative sampling (§ 3.3) is employed for each action. Every leaf node represents a complete action and is scored using a rule-based reward function. We then backpropagate the rewards along the tree to assign credit to intermediate reasoning steps. This process yields thinking-level contrastive pairs for DPO, which further improves the model's reasoning ability. The detailed process is presented in Algorithm 1.

3.1 Multi-turn Thinking Process Formulation

Each mobile GUI task contains a trajectory $\mathcal{T}$, several pages u, actions $\hat{a}$, and an instruction I, which can be represented as:

$$\mathcal{T} = \{I, u_0, \hat{a}_0, u_1, \hat{a}_1, \cdots, u_n, \hat{a}_n\} \tag{1}$$

We formulate action $\hat{a}_i$ in the CoaT reasoning process as a multi-turn dialogue $\hat{a}_i = [s_1, s_2, s_3, s_4]$, where s_i represents description, action-thought, action-decision, and grounding, respectively. This thinking paradigm based on the thinking–decision–grounding triplet, has been widely validated as effective in previous GUI works (Shen et al., 2024; Zhang et al., 2024b; Qin et al., 2025; Cheng et al., 2024). So the reasoning process can be formulated as:

$$s_1 = \text{Description}(P_1, u_i) \tag{2}$$

$$s_2 = \text{Thought}(P_2, u_i, I, \hat{a}_0, \cdots, \hat{a}_{i-1}, s_1) \tag{3}$$

P represents each round of dialogue input prompt, I is the task instruction, u is the current GUI, and $\hat{a}_i$ is the step i history action. Agents perform poorly when decoding the entire reasoning process in a single step, which is because image modal u dominates the input tokens, surpassing textual instructions I and action history $\hat{a}_i$, and diverting their attention away from the textual details. During autoregressive training, the agent is unaware that producing a final answer conforming to the required format is indispensable throughout the reasoning process. Multi-turn thinking process effectively mitigates this problem, because additional dialogue steps guarantee a final answer is generated:

$$s_3 = \text{Action}(P_3, u_i, I, s_1, s_2) \tag{4}$$

$$s_4 = \text{Grounding}(P_4, u_i, I, s_1, s_2, s_3) \tag{5}$$

Previous work either performed RL in GUI-Agent directly on the trajectory without CoaT, missing the detailed thinking process of each action, or forced the model to bear the heavy burden of outputting the entire reasoning process at once. In our method, when the reasoning process ends, the final s_4 is recorded as $\hat{a}_{n+1}$, step i moves one step forward on the trajectory $\mathcal{T}$ and its thinking step reward is calculated recursively based on final step s_4. Dialogue-level textual input helps balance cross-modal token proportions and steers the agent's attention toward the current reasoning step.

3.2 Instruction Evolution

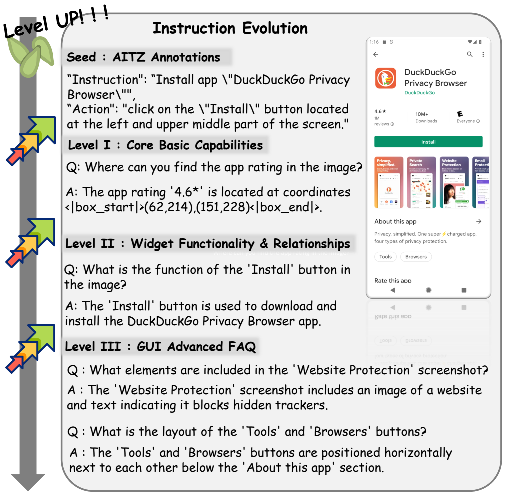

"Instruction": "Install app \"DuckDuckGo Privacy Browser\"",
"Action": "click on the \"Install\" button located at the left and upper middle part of the screen."

Q: Where can you find the app rating in the image?

A: The app rating '4.6*' is located at coordinates <|box_start|>(62,214),(151,228)<|box_end|>.

Q: What is the function of the 'Install' button in the image?

A: The 'Install' button is used to download and install the DuckDuckGo Privacy Browser app.

Q : What elements are included in the 'Website Protection' screenshot?

A : The 'Website Protection' screenshot includes an image of a website and text indicating it blocks hidden trackers.

Q : What is the layout of the 'Tools' and 'Browsers' buttons?

A : The 'Tools' and 'Browsers' buttons are positioned horizontally next to each other below the 'About this app' section.

Figure 2: We process a three-stage instruction evolution and knowledge augmentation, enabling the agent to produce more diverse outputs for corresponding tasks while effectively mitigating overfitting.

As discussed in the previous section, the CoaT patterns in the mobile agent domain are typically fixed. As a result, agents tend to overfit these static paradigms and struggle to generate diverse reasoning paths after the warm-up SFT training (as detailed in Sec 4.4). To address this issue, we enhance the original training trajectories, denoted as $\mathcal{T}$, by appending additional Q&A annotations to UI screenshots through an instruction evolution process, thereby creating a new dataset $\mathcal{Q}$ with a broader range of instruction formats. Specifically, as shown in Figure 2, the evolution process consists of three levels:

Level I: General GUI Q&A tasks. Grounding, Reference (Ref), and Page Descriptions are aimed at enhancing the agent's foundational capabilities. These tasks (Liu et al., 2024; Yang et al., 2024) are proven to be the core capabilities of GUI agents during the pre-training.

Level II: Widget caption and relationships. Descriptions of widget functions and the nested partition relationships between widgets. These tasks help agents understand the relationships between widgets, as previous work (Deng et al., 2024) has found that agents tend to click on the textview, even in scenarios where the textview and the button are separate.

Level III: GUI advanced FAQ. Inspired by Shen et al. (2024), we design an advanced FAQ that features more complex Q&A, including descriptions of the page's structural framework as well as expectations and predictions about navigation outcomes triggered by control interactions.

Warm-up Supervised Fine-tuning: To develop agents with standard thinking format and expand the reasoning space, we mix $\mathcal{T}$ and the instruction evolution data $\mathcal{Q}$, then perform warm-up SFT on $\mathcal{D} = \Big\{\mathcal{T}, \mathcal{Q}\Big\} = \Big\{(u, e)^{(i)}\Big\}_{i=1}^{|\mathcal{D}|}$, where u represents the prior knowledge (instructions, screenshot and action history) from $\mathcal{T}$ or the questions from $\mathcal{Q}$, and e is the reasoning process from $\mathcal{T}$ or the answer from $\mathcal{Q}$ which is organized into multi-turn dialogues. To ensure output diversity, we select an earlier checkpoint with better potential correct space and diverse output to serve as the seed policy model. More details can be seen in Appendix B.

3.3 Iterative Preference Learning

After the warm-up SFT, the agent acquires basic GUI capabilities. We construct a CoaT-tree by iteratively sampling each reasoning step and then assign a score to the leaf nodes based on a rule-based reward function. Using these scores, we generate thinking-level DPO pairs to optimize the agent's reasoning process.

Iterative Sampling & Rule-based Reward. We iteratively sample each reasoning step along the CoaT paradigm (Zhang et al., 2024b). The $\mathcal{K}$ sampling results $(\hat{s}_t|\hat{s}_{1:t-1})^{\mathcal{K}}$ at step t can be expressed as:

$$\hat{s}_t = \left\{ \left(\hat{s}_t^{(k)} \mid \hat{s}_0, \cdots, \hat{s}_{t-1} \right) \right\}_{k=1}^{K} \tag{6}$$

Naturally, the final step in CoaT (the leaf node in the sampling tree) expresses a reward compared with the ground truth action a^*, which is then propagated back to other intra-nodes. The formula for the rule-based reward of leaf nodes is as follows:

$$v(s_t) = \begin{cases} 1, & s_t = a* \\ v_{type} + score_{match}, & type(s_t \sim a^*) \\ 0, & others \end{cases} \tag{7}$$

$$score_{match} = \begin{cases} v_{format} + 1 \cdot (1 - d(x, y)) - (v_{type} + v_{format}) \cdot d(x, y), & type(a*) = CLICK \\ v_{format} + (1 - v_{type} - v_{format}) \cdot F_1, & type(a*) = INPUT \\ 0, & others \end{cases} \tag{8}$$

The reward score $v(s_t)$ ranges from 0 to 1, with a fully correct prediction receiving a score of 1. We use v_{type} and v_{format} to indicate whether the predicted action type and output format match the ground truth. For `click` and `input` actions, we further evaluate their internal structure using smooth rewards based on spatial distance $d(x, y)$ and text match F_1. The final reward is computed from the similarity between the prediction and the ground truth:

- **Click:** A distance-based score between the predicted and ground-truth coordinates, normalized to $[0, 1]$; smaller distances yield higher scores.
- **Input:** The F_1 score between the predicted and ground-truth strings; greater textual overlap yields higher scores.

The full reward is defined in Equation 7 and discussed further in Section C.

Based on the structure of the CoaT-tree, we recursively compute the value of each intermediate reasoning step. Specifically, the value of s_{t-1} is computed as the average value of its $\mathcal{K}$ sampled continuations at s_t:

$$v(s_{t-1}) = c \cdot \frac{1}{\mathcal{K}} \sum_{k=1}^{\mathcal{K}} v(s_t^{(k)}) \tag{9}$$

Here, $\mathcal{K}$ denotes the number of sampled continuations for each reasoning step, and c is a discount factor. The parameter searching experiment for $\mathcal{K}$ is described in detail in Section 4.4.

Contrastive Data Filter. After obtaining the sampling tree and node values, we evaluate the quality of the trees and extract contrastive data. We can divided the sampling trees into three categories $\mathcal{R} = \{\alpha, \beta, \gamma\}$ based on their output quality, and the classification standards of α, β, γ are as follows:

$$\alpha = \frac{\left| \left\{ \mathcal{S}^{(i)} \mid \forall v_k \in \mathcal{S}^{(i)}, v_k = 1 \right\} \right|}{\sum_{i=1}^{|\mathcal{T}|} |(u, e)^{(i)}|} \tag{10}$$

$$\beta = \frac{\left| \left\{ \mathcal{S}^{(i)} \mid \exists v_k, v_{k'} \in \mathcal{S}^{(i)}, v_k = 1, v_{k'} \neq 1 \right\} \right|}{\sum_{i=1}^{|\mathcal{T}|} |(u, e)^{(i)}|} \tag{11}$$

$$\gamma = \frac{\left| \left\{ \mathcal{S}^{(i)} \mid \forall v_k \in \mathcal{S}^{(i)}, v_k \neq 1 \right\} \right|}{\sum_{i=1}^{|\mathcal{T}|} |(u, e)^{(i)}|} \tag{12}$$

$\mathcal{S}^{(i)}$ and v_k refer to the instruction i sampling tree and the k-th leaf nodes value of $\mathcal{K}$ sampled output. α is considered a perfect sampling tree, which can stably output correct thoughts and actions with in-domain trajectories, β represents potential correct trees that can be used to construct contrastive data, and γ denotes sampling trees that require refinement. $\beta + \gamma$ is considered a valid sampling space. In β, actions with a value of 1 and as many diverse action types as possible are extracted as positive samples. In γ, the final ground truth action a^* is used as a positive sample, but the intermediate steps of CoaT are not provided, and the pairs can be represented as:

$$\begin{aligned} \beta_{pairs} = \langle \hat{s}_t^{(k)} \uparrow, \hat{s}_t^{(k')} \downarrow | \, (\hat{s}_1, \ldots, \hat{s}_{t-1}), \\ v(\hat{s}_t^{(k)}) - v(\hat{s}_t^{(k')}) > 1/\mathcal{K} \rangle \end{aligned} \tag{13}$$

$$\gamma_{pairs} = \langle a^* \uparrow, \hat{s}_t^{(k)} \downarrow | \, \hat{s}_1, \ldots, \hat{s}_{t-1} \rangle \tag{14}$$

Thinking-level Direct Preference Optimizing. After CoaT thinking-level Iterative Sampling, several positive and negative example pairs are collected. During this stage, the agent policy undergoes updates through the above data-pairs, SFT loss, and CoaT-DPO loss (Rafailov et al., 2023). Suppose the agent gets values to pair $\langle +, - \rangle$ at CoaT step t, which are named s_t^+ and s_t^-; we have the agent performing a comparison for these pairs based on the same thoughts $s_{1:t-1}$, which can be calculated as:

$$\begin{aligned} \mathcal{L}_{\text{T-DPO}} = -\mathbb{E}_{(s_{1:t-1}, s_t^-, s_t^+) \sim \mathcal{T}_s} \Bigg[\log \sigma \Big(\beta \log \frac{\pi_\theta(s_t^+ | s_{1:t-1})}{\pi_{ref}(s_t^+ | s_{1:t-1})} \\ - \beta \log \frac{\pi_\theta(s_t^- | s_{1:t-1})}{\pi_{ref}(s_t^- | s_{1:t-1})} \Big) \Bigg], \end{aligned} \tag{15}$$

To further refine the agent's performance post-optimization, we employ the updated agent as the new base agent to continue collecting contrastive CoaT-action level pairs for additional T-DPO training. This iterative process is maintained until the agent reaches the performance bottleneck.

Algorithm 1: Iterative CoaT thinking-level sampling and DPO self-training.

```
Input: base VLM $\pi$, advanced annotated model $R_{SoTA}$, step-level trajectory data $\mathcal{T}$, instruction evolution
    Q&A set $\mathcal{Q}$, number of sampling $\mathcal{K}$, golden action $a^*$, value function $v$, the sampled CoaT data $D$, number
    of iterations $\mathcal{N}$.
for $i = 1$ to $N_0$ do
    $\mathcal{Q}^* \leftarrow$ instruction_evolution($R_{\text{SoTA}}, \mathcal{T}$) // instruction evolution by GPT-4o
    $\mathcal{Q} \leftarrow$ human_evaluation($h, \mathcal{Q}^*$) // human filter
end for
$\pi_{S_0} \leftarrow$ Warm-up_SFT($\pi, \mathcal{T}, \mathcal{Q}$) // fine-tune seed model
for $n = 1$ to $\mathcal{N}$ do
    for $i = 1$ to $|\mathcal{T}|$ do
        $D_i \leftarrow$ generate_sampling_thought($\pi_{S_{n-1}}, \mathcal{T}_i, \mathcal{K}$) // CoaT Sampling
        $V_i^{leaf} \leftarrow v(D_i, a_i^*)$ // match and calculate leaf values using Eq(7)
        $V_i^{intra} \leftarrow$ recursive_calculate($D_i, V_i^{leaf}$) // recursive intra node values using Eq(9)
        $D_i^+, D_i^- \leftarrow$ contrastive_data_filter($D_i, V_i$) // filter positive and negative data using
        Eq(13, 14)
    end for
    $\pi_{S_n} \leftarrow$ DPO($\pi_{S_{k-1}}, D^+, D^-$) // DPO self-training reference model
end for
Output: $\pi_S, D_G, \mathcal{Q}$
```

4 Experiments

4.1 Experiments Setups

Dataset. AITZ (Zhang et al., 2024b) is a high-quality trajectory set filtered and re-annotated from AITW (Rawles et al., 2023), containing four subsets , which also includes five types of actions **AMEX** (Chai et al., 2024) uses the same apps and action space as AITZ, but its task instructions are more complex and detailed, with an average trajectory length of 15+. **AndroidControl** (Li et al., 2024a) includes OOD datasets, such as app unseen and task unseen.

Metrics. For evaluation, we use **Step.Acc** as metrics, consistent with Auto-GUI(Zhang & Zhang, 2023), measures the agent's performance and uses **Action Type** to assess the degree of action type matching. This metric effectively evaluates the model's planning ability.

Table 1: **Main results of AITZ dataset.** ZS, FT, PF, and IPL are short for zero-shot, fine-tuning, specific domain pre-training, and iterative preference learning, respectively. '-' represents that the agent or evaluation prompt is not open-sourced. Seed means the seed model for sampling and T-DPO training. R_i refers to the number of iterations during training.

Model	Mode	Atomic								
		SCROLL	CLICK		TYPE		PRESS	STOP	Total	
			type	match	type	match			type	match
CogAgent (CoaT)	ZS	70.22	88.23	66.15	45.80	21.80	45.95	24.60	72.59	53.28
AUTO-GUI (CoaT)	FT	61.40	74.56	32.20	87.20	81.40	57.70	74.40	82.98	47.69
AriaUI-MoE	FT	53.73	85.51	60.20	84.20	80.80	63.70	76.38	78.53	63.56
Seeclick-7B	PF	11.14	69.92	52.96	53.80	53.00	67.88	55.36	62.93	49.11
UGround-7B	PF	58.22	80.94	58.48	82.56	73.85	58.22	68.78	74.54	60.19
OS-Atlas-7B	PF	76.12	75.82	54.83	87.80	81.60	68.67	**81.75**	77.83	65.11
UI-Tars-7B	PF	52.50	83.03	64.27	**89.97**	82.76	61.87	74.35	77.59	65.61
Falcon-UI-7B	PF	-	-	-	-	-	-	-	**84.70**	69.10
Qwen2-VL-7B (CoaT)	FT	47.50	81.53	59.72	81.96	73.85	**58.22**	67.39	74.26	60.36
AITZ-Seed	FT	42.83	82.48	53.16	82.56	75.29	56.65	61.82	73.14	55.40
MobileIPL	IPL	51.08	**91.73**	**71.45**	88.20	**83.40**	51.69	78.17	81.90	**69.15**

Table 2: **Main results on AMEX**. Seed means the seed model for sampling.

Model	Training Data	Gmail	Booking	Music	SHEIN	News	CM	ToDo	Signal	Yelp	Overall
SeeClick-7B	AITW+External	28.2	29.4	18.1	20.0	30.0	53.1	30.7	37.1	27.4	30.44
SphAgent-7B	AITW	32.1	45.9	46.1	35.1	48.3	61.1	55.9	43.3	42.9	45.63
SphAgent-7B	AMEX	61.7	68.2	77.7	**72.0**	71.9	64.6	**79.6**	71.3	69.6	70.71
AriaUI-MoE	AMEX	63.1	62.3	68.5	58.9	83.0	54.7	62.5	83.3	66.9	64.10
UGround-7B	AMEX	70.9	68.8	72.7	63.7	77.7	67.7	63.7	80.1	67.6	69.12
SphAgent-7B	AITW + AMEX	62.4	68.1	76.3	71.9	68.6	67.3	77.6	66.0	64.1	69.14
OS-Atlas-7B	AMEX	61.1	**73.5**	77.9	61.6	75.2	66.4	71.0	75.9	72.0	70.33
UI-Tars-7B	AMEX	67.7	70.0	71.8	63.8	71.5	67.7	77.0	**86.4**	72.8	70.33
Qwen2-VL-7B	AMEX	58.0	70.1	76.6	63.8	79.4	66.8	67.8	80.2	**76.6**	69.01
	+ CoaT	75.9	68.1	77.7	66.2	76.8	66.4	77.5	79.6	65.6	70.93
MobileIPL-7B	AMEX (Seed)	57.0	60.2	68.8	63.1	75.0	50.2	65.6	77.7	62.6	62.19
	MobileIPL	**77.3**	71.8	**80.0**	68.4	**85.3**	**71.3**	73.5	82.1	71.8	**74.29**

Baselines. Following prior work(Wu et al., 2024)(Qin et al., 2025), we use Qwen2-VL-7B (Wang et al., 2024b) as the backbone of our model. We select CogAgent (Hong et al., 2024), AUTO-GUI, Shpagent, OS-Atlas, UGround, UI-Tars and FedMobileAgent as baseline agents. GUI continuous pre-training agents can be further divided into two categories: (1) training the model as a GUI grounding agent, such as OS-Atlas-7B. (2) training the model as a general GUI agent, such as UI-Tars. More details are provided in Appendix D.

4.2 Main result

AITZ. As shown in Table 1, MobileIPL achieves SoTA performance on most metrics. The reason for the lower PRESS Acc. is discussed in Section 4.4 and Appendix H. Multiple rounds of T-DPO improve MobileIPL by more than 10% (55.40% -> 69.15%) compared to the seed model MobileIPL and Qwen2-VL-7B (60.36% -> 69.15%). Compared to continuous pre-training agents such as Falcon-UI, which is pre-trained on three million GUIs, MobileIPL still surpasses a performance difference of 0.05%. The amount of training data required by our method is substantially smaller than that used by these pre-training approaches.

AMEX. As shown in Table 2, MobileIPL surpasses the previous SOTA model, SphAgent-7B, by 3.58%. It also outperforms the baseline model (Qwen2-vl+CoaT) by 3.36%. Additionally, MobileIPL surpasses OS-Atlas (+3.69%) and UI-Tars (+3.69%), both of which also use Qwen2-vl as the backbone. With the incorporation of CoaT, the baseline model Qwen2-vl shows an increase of 1.92%, demonstrating the effectiveness of CoaT patterns. In summary, these results confirm that MobileIPL delivers significant improvements over existing models in long trajectory scenarios.

Table 3: High-level instruction experiment results on **AndroidControl**.

Mode	Model	Grounding	Step.Acc
FT	Aria-UI-7B	43.2	10.2
	InternVL-2-4B	72.7	66.7
	Qwen2-VL-7B (SFT)	68.5	69.1
PF	OS-Atlas-7B	78.5	71.2
	Falcon-UI-7B	-	72.7
	UI-Tars-7B	**80.5**	72.5
RL	Qwen2-VL-7B(GRPO)	70.7	69.8
Ours	MobileIPL	77.0	**72.7**

Table 4: High-level instruction results on **AndroidControl in-domain** and **OOD** subsets.

Mode	Model	IDD	app-UN	task-UN
FT	PaLM 2S(full)	65.5	58.7	59.7
	PaLM 2S(LoRA)	70.8	58.5	59.6
	Qwen2-VL-7B(SFT)	69.1	61.4	64.1
PF	FedMobileAgent	54.7	52.3	51.2
	SphAgent-7B	69.4	57.1	62.9
	OS-Atlas-7B	71.2	60.7	66.2
RL	Qwen2-VL-7B(GRPO)	70.2	68.1	69.7
IPL	MobileIPL-7B	**73.6**	**70.0**	**72.2**

AndroidControl. As shown in Table 3, MobileIPL achieves SOTA performance in Step.Acc (72.7%), reaching the SOTA model Falcon-UI with fewer data. MobileIPL also outperforms continual pre-training agents in the GUI domain, such as OS-Atlas (+1.5%) and UI-Tars (+0.2%). Compared to the baseline model Qwen2-VL(SFT), MobileIPL not only improves Mobile Agent performance but also enhances grounding by 8.5%. As shown in Table 4, MobileIPL continues to achieve SOTA performance in unseen OOD settings, demonstrating strong generalization. In contrast, compared to performance in the IDD domain, the pre-trained model OS-Atlas shows a significant drop. MobileIPL exhibits less performance degradation in out-of-domain settings. We also ran GRPO with Qwen2-VL under the same computational resources, and found OOD performance similar to MobileIPL, because both are self-training. However, MobileIPL still outperforms GRPO in all subsets.

4.3 Ablation Study

To test the effectiveness of IPL and instruction evolution, we conducted ablation experiments. First, removing IPL and using only SFT caused performance to drop from 65.4% to 60.4%, compared to the first round of MobileIPL, highlighting the crucial role that IPL plays. Next, removing instruction evolution led to a 2.5% drop in IPL performance in the first round. This occurs because, without evolution, the model generates fewer training samples (156,418 -> 113,239). And as shown in Figure 3 (a), without instruction evolution, the diversity of model outputs decreased, causing a drop in IPL performance. This further confirms that instruction evolution is crucial for improving IPL.

Table 5: Ablation study results on AITZ.

Model	Scroll	Click	Type	Press	Total
MobileIPL-R1	45.8	71.1	81.2	23.5	65.4
- IPL	46.9	59.4	78.6	55.4	60.4 (-5.0)
- Evo (R1)	44.8	67.7	78.8	24.0	62.9 (-2.5)
- IPL Negative (R1)	46.9	61.1	74.2	56.6	61.4 (-4.0)
- IPL + Naive DPO (R1)	47.5	59.7	73.8	58.2	60.3 (-5.1)
- 1/2 training data (R1)	42.9	68.3	79.0	43.8	64.8 (-0.6)
- 4/5 training data (R2)	30.8	67.1	77.6	33.2	60.6 (-4.8)

Standard Self Training. Additionally, we remove negative samples from IPL-R1, training the model using only fully correct samples. This results in a 4.0% performance drop, suggesting that negative samples help the model learn how to reason rather than merely memorize (SFT). Furthermore, training on the entire trajectory with navie DPO reduces performance from 65.4% to 60.3%. Compared with SFT trained on CoaT tree positive data (–IPL Negative), naive DPO is still 1.1 % lower, confirming the effectiveness of CoaT-tree sampling and the thinking-process optimization.

Low Resource. We also perform low-resource on AITZ, sampling 1/2 and 1/5 of the training data. As shown in table 5, using only half of the data, the first round of IPL training already outperformed the best results achieved by the original CoAT-SFT (-IPL) and naive DPO training. Furthermore, when using only one-fifth of the data, the second round of IPL training surpassed the performance of CoAT-SFT (-IPL), demonstrating the effectiveness of our method even in low-resource scenarios.

4.4 Discussion and Analysis

Reasoning Space Sampling. To evaluate the instruction evolution, we analyze the diversity of the sampling space for **Random 1000 steps**, the standard deviation of encoded embeddings, the dimensionality-reduced distribution, and the distribution of $S^{(i)}$ mentioned in Section 3.3. As shown

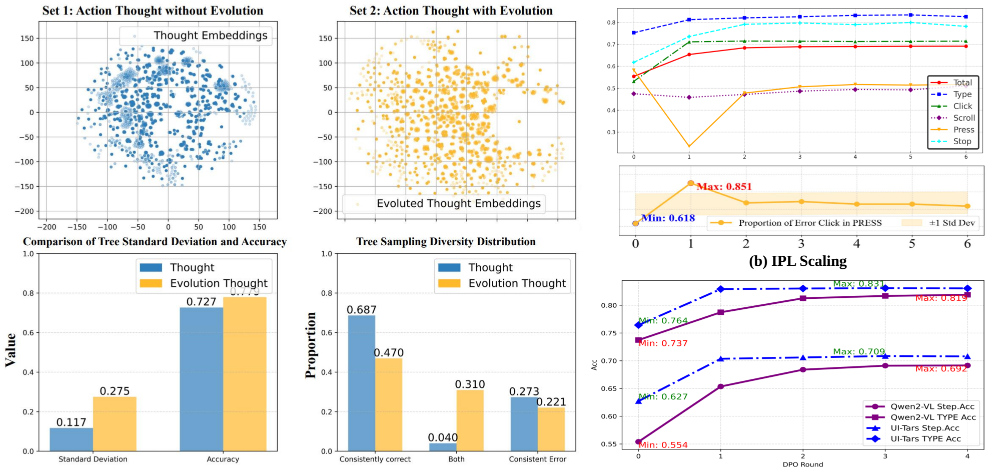

(a) Reasoning Space Sampling

(b) IPL Scaling

(c) IPL on Pre-training Agents

Figure 3: (a) Reasoning diversity before and after instruction evolution (left top) and the distribution of standard deviation and accuracy (left bottom). (b) **Step.Acc** changes for action types in AITZ across IPL iterations (right top). (c) The performance of UI-Tars-7B and Qwen2-VL-7B on AITZ as the seed model with 4-round IPL training (right bottom).

in Figure 3 (a), the thoughts after instruction evolution exhibit a broader space than direct SFT. Additionally, the embedding standard deviation within each tree increases significantly compared to the original data (+ 0.158). The diversified outputs do not negatively impact the agent's reasoning process, while the proportion of action sampling that includes the correct answer improves from 72.7% to 77.9%. The bottom-right subplot reflects the distribution of output accuracy. **Consistently Correct** indicates that all samples for the current step match the golden answer, while **Consistently Error** is the opposite. **Both** represents cases where some samples are correct while others are incorrect, which serves as an ideal source for constructing T-DPO pairs. Compared to 47% on the evolved data, the agent achieves 68.7% convergence on the original data but exhibits a strong polarization(4%). Three-stage instruction evolution significantly expands the sampling space (from 4% to 31%), proving that it simultaneously improves both the diversity and quality of reasoning. More details are in Appendix F.

Table 6: **Parameters Searching** on AITZ for the first round. $\mathcal{K}$ is the sampling number and R is the round of T-DPO learning.

Parameter	TYPE	CLICK	SCROLL	PRESS	STOP	Total
$\mathcal{K} = 2$	79.2	68.9	35.1	38.3	76.1	64.0
$\mathcal{K} = 3$	81.2	71.1	45.8	23.4	73.5	65.3 (**+1.3**)
$\mathcal{K} = 4$	81.2	70.4	51.2	35.5	66.8	65.9 (**+0.6**)
$R = 0$	75.7	53.3	43.7	58.2	63.2	57.5
$R = 1$	77.5	71.1	43.3	23.5	67.0	61.2 (**+3.7**)
$R = 2$	80.5	71.1	47.0	31.1	67.6	64.1 (**+2.9**)
$R = 3$	82.0	71.5	47.2	47.8	79.1	68.4 (**+4.3**)
$R = 4$	82.6	71.5	51.1	51.7	78.2	69.2 (**+0.8**)

Parameters Searching. We conducted an ablation study on the impact of the sampling number ($\mathcal{K}$) per stage and iterative round number (R). As shown in the table 6, increasing the number of samples generally leads to better model performance. However, since our framework adopts a tree structure, increasing the sampling number from 3 to 4 causes the minimum number of tree nodes to grow significantly from $3^3 = 27$ to $4^3 = 64$. Despite this sharp increase, the performance improvement is limited (less than 1%). Therefore, we adopt a sampling number of 3 for the final experiments. Regarding the number of rounds, we observe that both IPL performance and the size of the self-training dataset converge after several iterations. We therefore select the convergence round as our default setting. Additional details on computational cost are provided in Appendix G.

IPL Scaling. Although overall Step.Acc increases across IPL iterations, not all action types follow this trend. As shown in Figure 3(b), from the seed model to the first IPL round, PRESS accuracy drops sharply (58.22% → 23.49%), whereas CLICK rises (53.26% → 71.12%). In the second round, however, PRESS accuracy rebounds. This stems from the severe underrepresentation of PRESS actions early on: the proportion of PRESS samples in the preference data grows from 1.6% (1 round) to 10.9% (2 round) as training progresses. With greater reasoning diversity and more PRESS-related examples, the model gradually learns PRESS behaviors and recovers accuracy in later rounds.

Iterative Preference Learning On GUI Continuous Pre-training Agent. As discussed in the previous experimental analysis, continuous pre-training in the GUI domain provides the agents with a stronger base model. However, we still need to explore the compatibility between post-training IPL, instruction evolution, and pre-training. As shown in Figure 3 (c), UI-Tars outperforms Qwen2-VL-7B in all training stages, demonstrating better performance during the instruction evolution phase (62.7% > 55.4%). After four rounds of IPL, UI-Tars Step.Acc improves by 1.4% compared to MobileIPL (69.2% -> 70.6%). More importantly, UI-Tars nearly converges after the first round of IPL, significantly reducing the number of sampling and preference learning iterations, thereby keeping the computational cost of post-training within an acceptable range.

5 Conclusion

In this paper, we propose Mobile Iterative Preference Learning (**MobileIPL**), a self-training GUI agent framework that incorporates instruction evolution, iterative sampling in the CoaT-tree, and a rule-based reward. We extensively evaluate MobileIPL on the AITZ, AMEX, and AndroidControl benchmarks, demonstrating its effectiveness. Furthermore, MobileIPL exhibits strong generalization capabilities on the OOD subsets of AndroidControl. Experiments show that instruction evolution increases output diversity, generates more training data in IPL, and thereby improves IPL performance. Finally, Continuous Pre-training experiments confirm the mutual reinforcement between MobileIPL and pre-training, leading to enhanced performance.

6 Ethics Statement

We have rigorously refined our dataset to remove any elements that could compromise personal privacy, thereby guaranteeing the highest level of protection for individual data. Instruction evolution was completed by AI SoTA close-sourced VLM, to whom we paid the necessary compensation to ensure that the training data was not leaked. The human evaluation of our work was carried out through a meticulously randomized selection of IT professionals. This process ensured a gender-balanced and educationally diverse panel, reflecting a wide spectrum of perspectives and expertise.

7 Reproducibility statement

All models and datasets used in this paper are open-source. The full experimental setup is detailed in Appendix D. Unless noted, all experiments use the same settings. We describe compute resources in Appendix G. Overall, these practices make our results reproducible.

References

Josh Achiam, Steven Adler, Sandhini Agarwal, Lama Ahmad, Ilge Akkaya, Florencia Leoni Aleman, Diogo Almeida, Janko Altenschmidt, Sam Altman, Shyamal Anadkat, et al. Gpt-4 technical report. *ArXiv preprint*, abs/2303.08774, 2023. URL https://arxiv.org/abs/2303.08774.

Mohammad Gheshlaghi Azar, Zhaohan Daniel Guo, Bilal Piot, Rémi Munos, Mark Rowland, Michal Valko, and Daniele Calandriello. A general theoretical paradigm to understand learning from human preferences. In Sanjoy Dasgupta, Stephan Mandt, and Yingzhen Li (eds.), *International Conference on Artificial Intelligence and Statistics, 2-4 May 2024, Palau de Congressos, Valencia, Spain*, volume 238 of *Proceedings of Machine Learning Research*, pp. 4447–4455. PMLR, 2024. URL https://proceedings.mlr.press/v238/gheshlaghi-azar24a.html.

Gilles Baechler, Srinivas Sunkara, Maria Wang, Fedir Zubach, Hassan Mansoor, Vincent Etter, Victor Carbune, Jason Lin, Jindong Chen, and Abhanshu Sharma. Screenai: A vision-language model for UI and infographics understanding. In *Proceedings of the Thirty-Third International Joint Conference on Artificial Intelligence, IJCAI 2024, Jeju, South Korea, August 3-9, 2024*, pp. 3058–3068. ijcai.org, 2024. URL https://www.ijcai.org/proceedings/2024/339.

Hao Bai, Yifei Zhou, Jiayi Pan, Mert Cemri, Alane Suhr, Sergey Levine, and Aviral Kumar. Digirl: Training in-the-wild device-control agents with autonomous reinforcement learning. In Amir Globersons, Lester Mackey, Danielle Belgrave, Angela Fan, Ulrich Paquet, Jakub M. Tomczak, and Cheng Zhang (eds.), *Advances in Neural Information Processing Systems 38: Annual Conference on Neural Information Processing Systems 2024, NeurIPS 2024, Vancouver, BC, Canada, December 10 - 15, 2024*, 2024. URL http://papers.nips.cc/paper_files/paper/2024/hash/1704ddd0bb89f159dfe609b32c889995-Abstract-Conference.html.

Yuxiang Chai, Siyuan Huang, Yazhe Niu, Han Xiao, Liang Liu, Dingyu Zhang, Peng Gao, Shuai Ren, and Hongsheng Li. AMEX: Android multi-annotation expo dataset for mobile gui agents. *ArXiv preprint*, abs/2407.17490, 2024. URL https://arxiv.org/abs/2407.17490.

Kanzhi Cheng, Qiushi Sun, Yougang Chu, Fangzhi Xu, Yantao Li, Jianbing Zhang, and Zhiyong Wu. SeeClick: Harnessing gui grounding for advanced visual gui agents. *ArXiv preprint*, abs/2401.10935, 2024. URL https://arxiv.org/abs/2401.10935.

Shihan Deng, Weikai Xu, Hongda Sun, Wei Liu, Tao Tan, Jianfeng Liu, Ang Li, Jian Luan, Bin Wang, Rui Yan, et al. Mobile-Bench: An evaluation benchmark for llm-based mobile agents. *ArXiv preprint*, abs/2407.00993, 2024. URL https://arxiv.org/abs/2407.00993.

Tinghe Ding. MobileAgent: enhancing mobile control via human-machine interaction and sop integration. *ArXiv preprint*, abs/2401.04124, 2024. URL https://arxiv.org/abs/2401.04124.

Nicolai Dorka, Janusz Marecki, and Ammar Anwar. Training a vision language model as smartphone assistant. *ArXiv preprint*, abs/2404.08755, 2024. URL https://arxiv.org/abs/2404.08755.

Kawin Ethayarajh, Winnie Xu, Dan Jurafsky, and Douwe Kiela. Human-centered loss functions (halos). Technical report, Technical report, Contextual AI, 2023.

Boyu Gou, Ruohan Wang, Boyuan Zheng, Yanan Xie, Cheng Chang, Yiheng Shu, Huan Sun, and Yu Su. Navigating the digital world as humans do: Universal visual grounding for gui agents. *ArXiv preprint*, abs/2410.05243, 2024. URL https://arxiv.org/abs/2410.05243.

Daya Guo, Dejian Yang, Haowei Zhang, Junxiao Song, Ruoyu Zhang, Runxin Xu, Qihao Zhu, Shirong Ma, Peiyi Wang, Xiao Bi, et al. Deepseek-r1: Incentivizing reasoning capability in llms via reinforcement learning. *ArXiv preprint*, abs/2501.12948, 2025a. URL https://arxiv.org/abs/2501.12948.

Yiran Guo, Lijie Xu, Jie Liu, Dan Ye, and Shuang Qiu. Segment policy optimization: Effective segment-level credit assignment in rl for large language models. *arXiv preprint arXiv:2505.23564*, 2025b.

Wenyi Hong, Weihan Wang, Qingsong Lv, Jiazheng Xu, Wenmeng Yu, Junhui Ji, Yan Wang, Zihan Wang, Yuxiao Dong, Ming Ding, and Jie Tang. Cogagent: A visual language model for GUI agents. In *IEEE/CVF Conference on Computer Vision and Pattern Recognition, CVPR 2024, Seattle, WA, USA, June 16-22, 2024*, pp. 14281–14290. IEEE, 2024. doi: 10.1109/CVPR52733.2024.01354. URL https://doi.org/10.1109/CVPR52733.2024.01354.

Zhenyu Hou, Ziniu Hu, Yujiang Li, Rui Lu, Jie Tang, and Yuxiao Dong. Treerl: Llm reinforcement learning with on-policy tree search. *arXiv preprint arXiv:2506.11902*, 2025.

Kechen Jiao, Zhirui Fang, Jiahao Liu, Bei Li, Qifan Wang, Xinyu Liu, Junhao Ruan, Zhongjian Qiao, Yifan Zhu, Yaxin Xu, et al. Tcpo: Thought-centric preference optimization for effective embodied decision-making. In *Proceedings of the 2025 Conference on Empirical Methods in Natural Language Processing*, pp. 9585–9599, 2025.

Wei Li, William E. Bishop, Alice Li, Christopher Rawles, Folawiyo Campbell-Ajala, Divya Tyamagundlu, and Oriana Riva. On the effects of data scale on UI control agents. In Amir Globersons, Lester Mackey, Danielle Belgrave, Angela Fan, Ulrich Paquet, Jakub M. Tomczak, and Cheng Zhang (eds.), *Advances in Neural Information Processing Systems 38: Annual Conference on Neural Information Processing Systems 2024, NeurIPS 2024, Vancouver, BC, Canada, December 10 - 15, 2024*, 2024a. URL http://papers.nips.cc/paper_files/paper/2024/hash/a79f3ef3b445fd4659f44648f7ea8ffd-Abstract-Datasets_and_Benchmarks_Track.html.

Wei Li, William E. Bishop, Alice Li, Christopher Rawles, Folawiyo Campbell-Ajala, Divya Tyamagundlu, and Oriana Riva. On the effects of data scale on UI control agents. In Amir Globersons, Lester Mackey, Danielle Belgrave, Angela Fan, Ulrich Paquet, Jakub M. Tomczak, and Cheng Zhang (eds.), *Advances in Neural Information Processing Systems 38: Annual Conference on Neural Information Processing Systems 2024, NeurIPS 2024, Vancouver, BC, Canada, December 10 - 15, 2024*, 2024b. URL http://papers.nips.cc/paper_files/paper/2024/hash/a79f3ef3b445fd4659f44648f7ea8ffd-Abstract-Datasets_and_Benchmarks_Track.html.

Yanda Li, Chi Zhang, Wanqi Yang, Bin Fu, Pei Cheng, Xin Chen, Ling Chen, and Yunchao Wei. AppAgent-V2: Advanced agent for flexible mobile interactions. *ArXiv preprint*, abs/2408.11824, 2024c. URL https://arxiv.org/abs/2408.11824.

Yizhi Li, Qingshui Gu, Zhoufutu Wen, Ziniu Li, Tianshun Xing, Shuyue Guo, Tianyu Zheng, Xin Zhou, Xingwei Qu, Wangchunshu Zhou, et al. Treepo: Bridging the gap of policy optimization and efficacy and inference efficiency with heuristic tree-based modeling. *arXiv preprint arXiv:2508.17445*, 2025.

Xiao Liu, Bo Qin, Dongzhu Liang, Guang Dong, Hanyu Lai, Hanchen Zhang, Hanlin Zhao, Iat Long Iong, Jiadai Sun, Jiaqi Wang, et al. AutoGLM: Autonomous foundation agents for guis. *ArXiv preprint*, abs/2411.00820, 2024. URL https://arxiv.org/abs/2411.00820.

Quanfeng Lu, Wenqi Shao, Zitao Liu, Fanqing Meng, Boxuan Li, Botong Chen, Siyuan Huang, Kaipeng Zhang, Yu Qiao, and Ping Luo. GUI Odyssey: A comprehensive dataset for cross-app gui navigation on mobile devices. *ArXiv preprint*, abs/2406.08451, 2024. URL https://arxiv.org/abs/2406.08451.

Trung Quoc Luong, Xinbo Zhang, Zhanming Jie, Peng Sun, Xiaoran Jin, and Hang Li. ReFT: Reasoning with reinforced fine-tuning. *ArXiv preprint*, abs/2401.08967, 2024. URL https://arxiv.org/abs/2401.08967.

Runliang Niu, Jindong Li, Shiqi Wang, Yali Fu, Xiyu Hu, Xueyuan Leng, He Kong, Yi Chang, and Qi Wang. Screenagent: A vision language model-driven computer control agent. In *Proceedings of the Thirty-Third International Joint Conference on Artificial Intelligence, IJCAI 2024, Jeju, South Korea, August 3-9, 2024*, pp. 6433–6441. ijcai.org, 2024. URL https://www.ijcai.org/proceedings/2024/711.

Songqin Nong, Jiali Zhu, Rui Wu, Jiongchao Jin, Shuo Shan, Xiutian Huang, and Wenhao Xu. MobileFlow: A multimodal llm for mobile gui agent. *ArXiv preprint*, abs/2407.04346, 2024. URL https://arxiv.org/abs/2407.04346.

Yujia Qin, Yining Ye, Junjie Fang, Haoming Wang, Shihao Liang, Shizuo Tian, Junda Zhang, Jiahao Li, Yunxin Li, Shijue Huang, et al. UI-TARS: Pioneering automated gui interaction with native agents. *ArXiv preprint*, abs/2501.12326, 2025. URL https://arxiv.org/abs/2501.12326.

Kevin Qinghong Lin, Linjie Li, Difei Gao, Zhengyuan Yang, Shiwei Wu, Zechen Bai, Weixian Lei, Lijuan Wang, and Mike Zheng Shou. ShowUI: One vision-language-action model for gui visual agent. *arXiv e-prints*, pp. arXiv–2411, 2024.

Rafael Rafailov, Archit Sharma, Eric Mitchell, Christopher D. Manning, Stefano Ermon, and Chelsea Finn. Direct preference optimization: Your language model is secretly a reward model. In Alice Oh, Tristan Naumann, Amir Globerson, Kate Saenko, Moritz Hardt, and Sergey Levine (eds.), *Advances in Neural Information Processing Systems 36: Annual Conference on Neural Information Processing Systems 2023, NeurIPS 2023, New Orleans, LA, USA, December 10 - 16, 2023*, 2023. URL http://papers.nips.cc/paper_files/paper/2023/hash/a85b405ed65c6477a4fe8302b5e06ce7-Abstract-Conference.html.

Christopher Rawles, Alice Li, Daniel Rodriguez, Oriana Riva, and Timothy P. Lillicrap. Androidinthewild: A large-scale dataset for android device control. In Alice Oh, Tristan Naumann, Amir Globerson, Kate Saenko, Moritz Hardt, and Sergey Levine (eds.), *Advances in Neural Information Processing Systems 36: Annual Conference on Neural Information Processing Systems 2023, NeurIPS 2023, New Orleans, LA, USA, December 10 - 16, 2023*, 2023. URL http://papers.nips.cc/paper_files/paper/2023/hash/bbbb6308b402fe909c39dd29950c32e0-Abstract-Datasets_and_Benchmarks.html.

John Schulman, Filip Wolski, Prafulla Dhariwal, Alec Radford, and Oleg Klimov. Proximal policy optimization algorithms. *ArXiv preprint*, abs/1707.06347, 2017. URL https://arxiv.org/abs/1707.06347.

Huawen Shen, Chang Liu, Gengluo Li, Xinlong Wang, Yu Zhou, Can Ma, and Xiangyang Ji. Falcon-UI: Understanding gui before following user instructions. *ArXiv preprint*, abs/2412.09362, 2024. URL https://arxiv.org/abs/2412.09362.

Q Team. Qwen2. 5-vl, january 2025. *URL https://qwenlm. github. io/blog/qwen2*.

Bryan Wang, Gang Li, and Yang Li. Enabling conversational interaction with mobile UI using large language models. In Albrecht Schmidt, Kaisa Väänänen, Tesh Goyal, Per Ola Kristensson, Anicia Peters, Stefanie Mueller, Julie R. Williamson, and Max L. Wilson (eds.), *Proceedings of the 2023 CHI Conference on Human Factors in Computing Systems, CHI 2023, Hamburg, Germany, April 23-28, 2023*, pp. 432:1–432:17. ACM, 2023. doi: 10.1145/3544548.3580895. URL https://doi.org/10.1145/3544548.3580895.

Junyang Wang, Haiyang Xu, Haitao Jia, Xi Zhang, Ming Yan, Weizhou Shen, Ji Zhang, Fei Huang, and Jitao Sang. Mobile-agent-v2: Mobile device operation assistant with effective navigation via multi-agent collaboration. In Amir Globersons, Lester Mackey, Danielle Belgrave, Angela Fan, Ulrich Paquet, Jakub M. Tomczak, and Cheng Zhang (eds.), *Advances in Neural Information Processing Systems 38: Annual Conference on Neural Information Processing Systems 2024, NeurIPS 2024, Vancouver, BC, Canada, December 10 - 15, 2024*, 2024a. URL http://papers.nips.cc/paper_files/paper/2024/hash/0520537ba799d375b8ff5523295c337a-Abstract-Conference.html.

Peng Wang, Shuai Bai, Sinan Tan, Shijie Wang, Zhihao Fan, Jinze Bai, Keqin Chen, Xuejing Liu, Jialin Wang, Wenbin Ge, et al. Qwen2-vl: Enhancing vision-language model's perception of the world at any resolution. *ArXiv preprint*, abs/2409.12191, 2024b. URL https://arxiv.org/abs/2409.12191.

Taiyi Wang, Zhihao Wu, Jianheng Liu, Jianye Hao, Jun Wang, and Kun Shao. DistRL: An asynchronous distributed reinforcement learning framework for on-device control agents. *ArXiv preprint*, abs/2410.14803, 2024c. URL https://arxiv.org/abs/2410.14803.

Wenhao Wang, Zijie Yu, William Liu, Rui Ye, Tian Jin, Siheng Chen, and Yanfeng Wang. FedMobileAgent: Training mobile agents using decentralized self-sourced data from diverse users. *ArXiv preprint*, abs/2502.02982, 2025. URL https://arxiv.org/abs/2502.02982.

Hao Wen, Yuanchun Li, Guohong Liu, Shanhui Zhao, Tao Yu, Toby Jia-Jun Li, Shiqi Jiang, Yunhao Liu, Yaqin Zhang, and Yunxin Liu. Empowering llm to use smartphone for intelligent task automation. *ArXiv preprint*, abs/2308.15272, 2023. URL https://arxiv.org/abs/2308.15272.

Qinzhuo Wu, Wei Liu, Jian Luan, and Bin Wang. ReachAgent: Enhancing mobile agent via page reaching and operation. *ArXiv preprint*, abs/2502.02955, 2025. URL https://arxiv.org/abs/2502.02955.

Zhiyong Wu, Zhenyu Wu, Fangzhi Xu, Yian Wang, Qiushi Sun, Chengyou Jia, Kanzhi Cheng, Zichen Ding, Liheng Chen, Paul Pu Liang, et al. Os-Atlas: A foundation action model for generalist gui agents. *ArXiv preprint*, abs/2410.23218, 2024. URL https://arxiv.org/abs/2410.23218.

Yuxi Xie, Anirudh Goyal, Wenyue Zheng, Min-Yen Kan, Timothy P. Lillicrap, Kenji Kawaguchi, and Michael Shieh. Monte carlo tree search boosts reasoning via iterative preference learning. *ArXiv preprint*, abs/2405.00451, 2024. URL https://arxiv.org/abs/2405.00451.

Yiheng Xu, Zekun Wang, Junli Wang, Dunjie Lu, Tianbao Xie, Amrita Saha, Doyen Sahoo, Tao Yu, and Caiming Xiong. Aguvis: Unified pure vision agents for autonomous gui interaction. *ArXiv preprint*, abs/2412.04454, 2024. URL https://arxiv.org/abs/2412.04454.

Yuhao Yang, Yue Wang, Dongxu Li, Ziyang Luo, Bei Chen, Chao Huang, and Junnan Li. Aria-UI: Visual grounding for gui instructions. *ArXiv preprint*, abs/2412.16256, 2024. URL https://arxiv.org/abs/2412.16256.

Zhao Yang, Jiaxuan Liu, Yucheng Han, Xin Chen, Zebiao Huang, Bin Fu, and Gang Yu. AppAgent: Multimodal agents as smartphone users. *ArXiv preprint*, abs/2312.13771, 2023. URL `https://arxiv.org/abs/2312.13771`.

Keen You, Haotian Zhang, Eldon Schoop, Floris Weers, Amanda Swearngin, Jeffrey Nichols, Yinfei Yang, and Zhe Gan. Ferret-UI: Grounded mobile ui understanding with multimodal llms. *ArXiv preprint*, abs/2404.05719, 2024. URL `https://arxiv.org/abs/2404.05719`.

Dan Zhang, Sining Zhoubian, Ziniu Hu, Yisong Yue, Yuxiao Dong, and Jie Tang. Rest-mcts*: LLM self-training via process reward guided tree search. In Amir Globersons, Lester Mackey, Danielle Belgrave, Angela Fan, Ulrich Paquet, Jakub M. Tomczak, and Cheng Zhang (eds.), *Advances in Neural Information Processing Systems 38: Annual Conference on Neural Information Processing Systems 2024, NeurIPS 2024, Vancouver, BC, Canada, December 10 - 15, 2024*, 2024a. URL `http://papers.nips.cc/paper_files/paper/2024/hash/76ec4dc30e9faaf0e4b6093eaa377218-Abstract-Conference.html`.

Jiwen Zhang, Jihao Wu, Yihua Teng, Minghui Liao, Nuo Xu, Xiao Xiao, Zhongyu Wei, and Duyu Tang. Android in the Zoo: Chain-of-action-thought for gui agents. *ArXiv preprint*, abs/2403.02713, 2024b. URL `https://arxiv.org/abs/2403.02713`.

Li Zhang, Shihe Wang, Xianqing Jia, Zhihan Zheng, Yunhe Yan, Longxi Gao, Yuanchun Li, and Mengwei Xu. LlamaTouch: A faithful and scalable testbed for mobile ui task automation. *ArXiv preprint*, abs/2404.16054, 2024c. URL `https://arxiv.org/abs/2404.16054`.

Zhuosheng Zhang and Aston Zhang. You only look at screens: Multimodal chain-of-action agents. *ArXiv preprint*, abs/2309.11436, 2023. URL `https://arxiv.org/abs/2309.11436`.

Boyuan Zheng, Boyu Gou, Jihyung Kil, Huan Sun, and Yu Su. Gpt-4v(ision) is a generalist web agent, if grounded. In *Forty-first International Conference on Machine Learning, ICML 2024, Vienna, Austria, July 21-27, 2024*. OpenReview.net, 2024. URL `https://openreview.net/forum?id=piecKJ2DlB`.

A CoaT Thinking Process

The table 7 summarizes the CoT paradigms (inputs and outputs) used in prior related works. CoaT paradigm for fine-tuning agents: The effectiveness of the approach in AITZ stems from the inclusion of extra screen descriptions as part of the input, along with joint output of Screen Context, Action Think, Action Target, and Action Result. In contrast, our experiments show that a stage-wise multi-turn dialogue output leads to better performance. In this setup, the model focuses on a single sub-task at each stage, which not only improves clarity but also encourages a simplified and deliberate reasoning process. This insight aligns with UI-TARS, which only requires the model to generate a brief thought during inference. Small-scale agent framing: Even models with relatively small parameter sizes can benefit from task-decomposed downstream training. For instance, OS-ATLAS and Falcon-UI adopt a similar architecture using GPT-4o for textual description and OS-ATLAS-base as the grounding model. They fine-tune models separately on different downstream tasks, resulting in a collection of OS-ATLAS-pro models, each specialized for a specific sub-task. Large-scale prompting-based frameworks: Larger models typically adopt a multi-agent framework to support a CoT-style reasoning process. For example, AppAgent v2 and Mobile-Agent-v2 both utilize a plan–action–reflection architecture to complete tasks. In our work, we adopt a stage-wise CoaT multi-turn dialogue format, where the model focuses on one sub-task at a time. This design enables us to move away from the dependence on extra screen description inputs, as seen in AITZ, while leveraging the description + grounding structure proposed in OS-ATLAS to form the final structure of the MobileIPL CoaT paradigm.

B Selection of Seed Policy Model

In our preliminary experimental exploration, we discovered that for the seed policy model, better performance in the SFT phase does not necessarily translate to a higher upper bound in the subsequent IPL phase. This is because as training progresses, the model's output space becomes increasingly

Table 7: Comparison of methods and their corresponding CoT paradigms.

Method	Backbone	Input	Output (CoT Paradigm)
Android in the Zoo	One fine-tuned agent	Instruction + image + screen description	Screen Context → Action Think → Action Target → Action Result
UI-TARS	One fine-tuned agent	Instruction + image	Thought → Action
OS-ATLAS	One fine-tuned agent + one large agent	Instruction + image	Action Description + Action Model
Mobile-Agent-v2	Multi-agent + prompt engineering	Instruction + image	Stage 1: Plan → Stage 2: Action → Stage 3: Reflection
MobileIPL	One fine-tuned agent	Instruction + image	Stage 1: Description → Stage 2: Plan → Stage 3: Action → Stage 4: Grounding

aligned with the training data, reducing its diversity in sampling. Consequently, for incorrect instances, the model tends to generate erroneous outputs regardless of the sampling attempts. To address this, we propose a sampling-oriented selection method for the seed policy model, incorporating the following two evaluation metrics:

Sampling Accuracy(Acc_S), which requires the model to hit more correct actions a in the sampled output space $\mathcal{S}$.

$$Acc_S = \frac{\sum_{i=1}^{|\mathcal{T}|} \left|\left\{e_j^{(i)} \mid a^{(i)} \sim e_j^{(i)}, e_j^{(i)} \in \mathcal{S}^{(i)}\right\}\right|}{\sum_{i=1}^{|\mathcal{T}|} |\mathcal{S}^{(i)}|} \tag{16}$$

Sampling Diversity(Div_R), which requires the model to have a more diverse and extensive sampling space. Standard deviation calculation of a single sampled tree $\mathcal{D}ev_{S^{(i)}}$:

$$Dev_{S^{(i)}} = \frac{1}{T} \sum_{t=1}^{T} \text{StdDev}\left(\mathbf{E}(\hat{s}_t^{(k)}) \mid k = 1, \ldots, \mathcal{K}\right) \tag{17}$$

Among them, $\mathbf{E}(\hat{s}_t^{(k)})$ represents the representation of the kth sample output of the tth step after the encoder. Calculation of the standard deviation of the set Div_S:

$$Div_R = \frac{1}{N} \sum_{i=1}^{N} Dev_{S^{(i)}} \tag{18}$$

where N is the number of sampled trees in the set $\mathcal{R}$.

C Rule-based Reward Design

Derivation Of The Value Function. Our value function incorporates hyperparameters inspired by ReFT and is also influenced by the sampling number used during IPL. We explain the rationale behind key parameter choices in our method, especially those in Eq.(7), Eq.(13), and Eq.(14):

Strong Reward: We follow the ReFT (Luong et al., 2024) score to define strong reward signals, assigning values of 1 and 0, corresponding to fully correct and completely incorrect reasoning paths, respectively. In ReFT, a supervision signal of 0.1 encourages the model to produce a final answer following the predefined format. In our approach, this signal is repurposed to reward action type matching. Meanwhile, an additional v_{format} reward is introduced to encourage proper formatting of actions.

Weak Reward: For input action, the value linearly increases from $v_{format} + v_{type}$ up to the strong reward level, with v_{format} acting as a threshold to distinguish weak from type-correct reward. For grounding actions, values range between $v_{format} + v_{type}$ and 1, too. A value of v_{format} indicates minimal correctness (e.g., extractable coordinates), while 1 indicates a closest match with the golden action, suitable for DPO pairing. Except v_{format} and v_{type} serving as discrete supervision signals, all other value signals are maintained as continuous. 1 / $\mathcal{K}$ in Eq. (13) arises naturally from our hierarchical training structure. For example, if one child is incorrect (e.g., value drops from 1 to 0), the average value for the parent node decreases by 0.33 when the sampling number is 3. Thus, 1 / $\mathcal{K}$ serves as a meaningful threshold to distinguish positive vs. negative examples in the CoAT tree.

Table 8: Text F1 vs. text-embedding similarity: ablation on reward design. Best results are in **bold**.

Reward Type	TYPE (type)	TYPE (acc)	TOTAL (type)	TOTAL (acc)
BERT	84.17	76.70	77.81	62.49
F1	**87.78**	**81.23**	**78.74**	**65.37**

Text F1 vs. Text-Embedding Similarity: We replaced the F1-based reward with a BERT-based semantic reward and evaluated both variants. As shown in Table 8, the F1 reward outperforms the BERT embedding reward across all metrics, with the largest gain on *TYPE ACTION (acc)* (+4.53%). This aligns with the importance of exact keyword matching in GUI input, indicating that F1 is better suited than semantic similarity for reward design in mobile UI input scenarios.

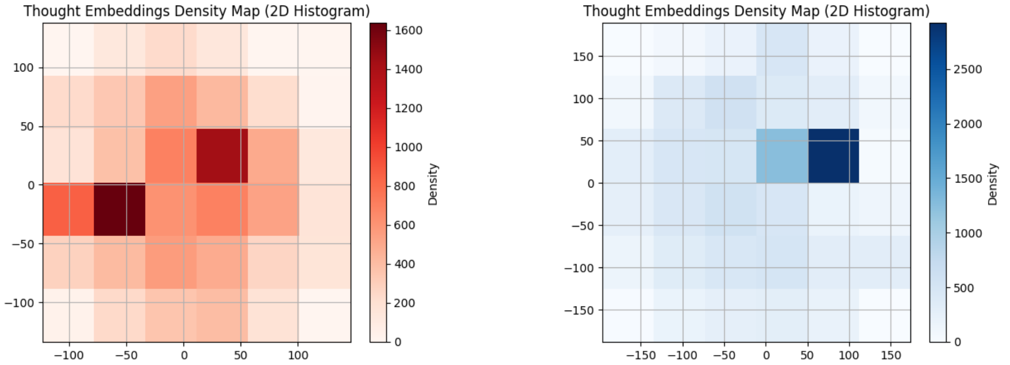

Figure 4: The heatmap at the left represents the sampling before instruction evolution, while the one at the right represents the sampling after instruction evolution.

D Experiment Setup

Models. Unlike AITZ, we do not compare the CoaT result with the expected page and decide whether to roll back because most actions in real-device scenarios cannot be rolled back without cost. Previous work conducted continual pretraining on Qwen2-VL-7B using GUI domain data, resulting in a stronger base model. In our ablation study, we discuss the impact of continuous pretraining on IPL. ()

Setup. We conduct hyperparameter searches on AITZ to reproduce the baseline results and find that the optimal learning rate ranges from 3e-5 to 3e-6. Therefore, all baseline fine-tuning experiments adopt this setting. Before IPL, during the instruction evolution stage, we apply LoRA fine-tuning with a LoRA rank of 128. For IPL Stage 1, we use a learning rate between 1e-6 and 1e-7. In subsequent stages, we apply a constant learning rate of 1e-7. The batch size is consistently set to 128. During fine-tuning (including baseline fine-tuning), we enable ViT training, whereas in the IPL phase, we experiment with freezing ViT. For AITZ training, we followed the Falcons' approach, utilizing a maximum 1540×1540 resolution. For other experiments, we reduce the resolution to 1280×720 to optimize computational efficiency. The maximum context length is set to 32K for all experiments. The fine-tuning experiments are conducted for 2 epochs, while IPL training is performed for 1 epoch. Since the large volume of Android control data, we sample 1/5 of the dataset for each IPL training iteration.

CoaT Multi-turn Dialogue Prompts.

1. **Page Description.** *Based on the mobile screenshot: Image URL, identify and describe the key elements visible on the screen, including any text, buttons, icons, input fields, or other interactive components.*

2. **CoaT Action Thought.** *Given the task: instruction, and considering the contextual details from the image alongside the full history of previous actions: action history, determine the most logical and effective next step. Focus on providing a clear, actionable, and goal-oriented response to advance the task.*

3. **CoaT Action Description.** *Task: Determine the Most Appropriate Next Step. Based on the previous analysis and the objective, determine the most appropriate next step to achieve the goal. Choose from the following options: - **click**: Select a button or specific UI element by specifying it clearly (e.g., 'click xxx', where 'xxx' is the button name or identifier). - **scroll**: Perform a scrolling action if the required element is not visible, specifying the direction (e.g., 'scroll up', 'scroll down'). - **type**: Input specific text into a field or search bar, specifying the text clearly (e.g., type "content"). - **press**: Interact with device-level buttons such as Home, Back, or Enter, specifying the button (e.g., "press Back"). - **stop**: Conclude the task, indicating that the objective has been achieved. Provide the chosen action in the specified format and ensure it aligns with the analysis and the visible UI elements.*

4. **Click Action Grounding.** *As discussed earlier, your task now is to identify the precise screen region coordinates to tap for the action coat action. The coordinates must be integers and strictly within the range of 0 to 1000 for both axes. Please provide your response in the required format: <|box_start|>(top_x, top_y),(bottom_x, bottom_y)<|box_end|>. Ensure your output adheres to these constraints and remains concise.*

Instruction evolution Prompts.

1. **Page Description Annotation.** *I will provide you with a mobile page. Please describe the current page. Your description should include the content of the page and its general functionality. Please note that the descriptions you generate should be of moderate length. Your page description should match the actual image.*

2. **Action Thought Annotation.** ***QUERY**: task, **ACTION HISTORY**: To proceed with the query, your past actions include: action history, **NEXT ACTION**: This is the next action you need to take: coat action, **TASK**: Given the screen and the above information, you have three tasks to do. First, you have to analyze what you have done. Second, you should analyze the screen for relevant details that might pertain to the given query. This includes checking for specific applications, icons, or buttons that are visible and any information or results that are currently displayed on the screen. Tip: If the screen does not have the information you need, you can scroll left or scroll up to try to get the information. Don't answer this logic question by saying that because the provided **NEXT ACTION** is..., therefore, the next action is... You need to think carefully on your own. You must answer the question with suitable lengths and the following format: 'Think: I have done..., Current screen is..., I need to... So the next action is ...' Your final action should be the same as the NEXT ACTION above.*

3. **Q&A Annotation.** *Your goal is to draw inspiration from the given images and image description information to create multiple new questions and answers. This new creation is closely related to the given image and information, but the answers involved should be directly derived from the given information, because UI positions and UI text are one-to-one correspondence. Specifically, you should construct the following three types of questions and answers, a total of 15: 1. the function of some elements in the image. 2. Grounding questions and answers (the coordinates and approximate location of the target in the image). 3. Partial detailed information questions and answers (the structural relationship between multiple elements, type, style, etc.). Please try to keep your questions and answers diverse and informative, and ignore the message in the device status bar. Here is the information related to the image: UI positions: {ui positions}, UI text: {ui text}, coat screen desc: {coat screen desc}, Please provide the following information in JSON format with the key questions and answers, and Don't add annotation parsing:*

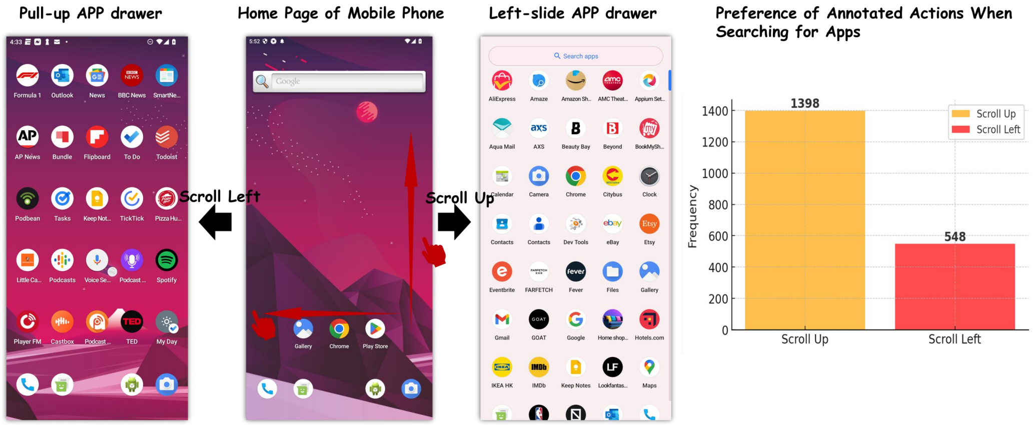

Figure 5: The left figure shows an example of unstable annotation preferences in **AMEX**, while the right figure presents the proportion of this type of annotation.

E Human Annotation

SoTA Model Cost: We use GPT-4o for annotation, which is priced at 4 USD per 1M input tokens and 16 USD per 1M output tokens. As shown in Appendix B (Instruction Evolution Prompts), each image has a resolution of 1080 × 2440. The input prompt is approximately 2K tokens, and the output is around 0.5K tokens, resulting in a per-page annotation cost of 0.008 USD (input) + 0.004 USD (output) = 0.012 USD. Given that the Android in the Zoo dataset [1] contains around 18,000 pages, the total annotation cost is approximately 200 USD.

Human Verification: Human verification is used to identify cases where the model produces incorrect thoughts due to being forced to align with the golden action. As shown in following table, some initial annotations contain template-like phrases (e.g., “Since”, “annotation”) and mention multiple possible actions. These mistakes often happen when the model tries to justify a given action even if it doesn’t match the actual screen.

The bolded text in following Table highlights common errors. To address this, we regenerated the prompts and applied automatic filtering based on specific tokens, which helps reduce the need for manual work.

Before Human Verification: "coat_action_think": "Reason for the Action: - To find and compare prices, the user needs to locate similar products. - Swiping up or scrolling down is a logical step to explore further information or discover additional options, as apps like Etsy often display "similar items" or "recommended products" below the primary product listing. - This action aligns with typical app design patterns where related items or comparison options are placed further down the page. 4. Logical Derivation of Action: - Since the task specifies comparing prices of similar items, and the current screen does not explicitly list such items, the user must navigate downward to uncover more options. - The instruction to "swipe up" (or scroll down) matches the action type ("action_type": "scroll", "direction""down"), indicating an attempt to reveal additional content or sections. 5. **Since the next action swiping down matches the annotation, the next action is swiping down**.

After Human Verification: Think: I have previously navigated "Back," which indicates that I may have returned to the previous screen or listing, likely as part of exploring options related to the query for comparing prices of men’s athletic shoes. Current screen is displaying detailed information about a product on the Etsy app. This includes item details such as "Handmade item," "Made to order," and shipping information. There are also options to "Follow shop," "Message seller," and "Add to cart," but it does not appear to directly show other comparable items or prices for similar men’s athletic shoes.I need to scroll further down on this screen to potentially uncover additional details, such as related products, a comparison section, or other useful information for the query. So the Next action is Scroll down."

Table 9: Data size and training time across iterative rounds.

	Standard SFT	Round 1	Round 2	Round 3	Round 4	Round 5
Data Samples	63,158	156,418	34,010	28,491	17,027	17,780
Time (hours)	2.8	7.9	2.0	1.7	1.0	1.0

F Iterative Sampling in the CoaT-tree

As shown in Figure 4, before instruction evolution, the distribution is highly concentrated, with only 8 points exceeding 1000 (including 3 points above 1200). After instruction evolution, the distribution becomes more balanced, with 20 points exceeding 1000 (including 2 points above 1500).

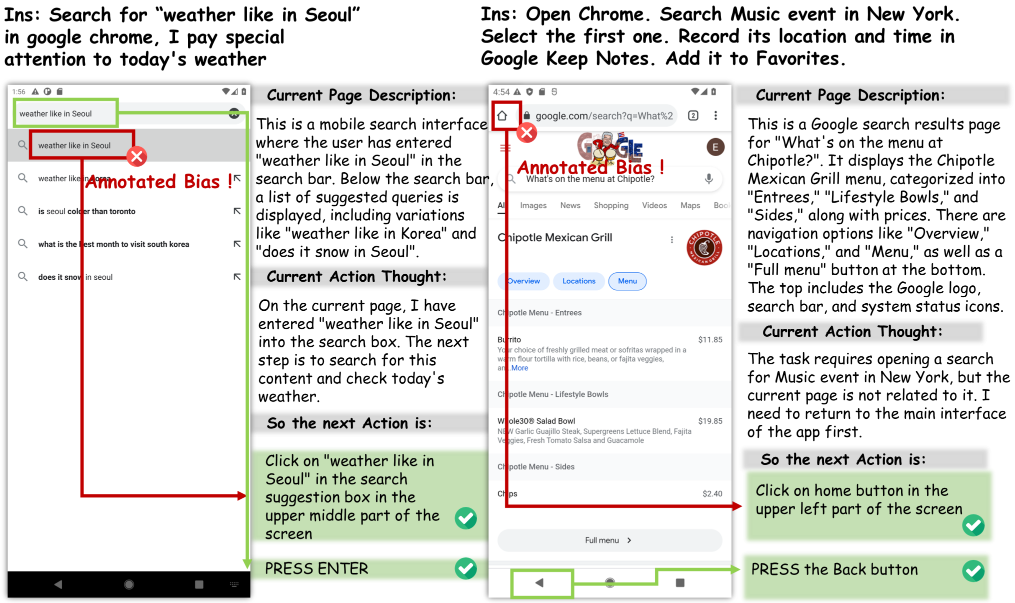

Ins: Search for "weather like in Seoul" in google chrome, I pay special attention to today's weather

Current Page Description:

This is a mobile search interface where the user has entered "weather like in Seoul" in the search bar. Below the search bar, a list of suggested queries is displayed, including variations like "weather like in Korea" and "does it snow in Seoul".

Current Action Thought:

On the current page, I have entered "weather like in Seoul" into the search box. The next step is to search for this content and check today's weather.

So the next Action is:

Click on "weather like in Seoul" in the search suggestion box in the upper middle part of the screen ✓

PRESS ENTER ✓

Ins: Open Chrome. Search Music event in New York. Select the first one. Record its location and time in Google Keep Notes. Add it to Favorites.

4:54
google.com/search?q=What%2
Annotated Bias !
What's on the menu at Chipotle?
All
Images
News
Shopping
Videos
Maps
Boo
Chipotle Mexican Grill
Overview
Locations
Menu
Chipotle Menu - Entrees
Burrito
$11.85
Your choice of freshly grilled meat or sofritas wrapped in a warm flour tortilla with rice, beans, or fajita veggies, and...More
Chipotle Menu - Lifestyle Bowls
Whole30® Salad Bowl
$19.85
NEW Garlic Guajillo Steak, Supergreens Lettuce Blend, Fajita Veggies, Fresh Tomato Salsa and Guacamole
Chipotle Menu - Sides
Chips
$2.40
Full menu

Current Page Description:

This is a Google search results page for "What's on the menu at Chipotle?". It displays the Chipotle Mexican Grill menu, categorized into "Entrees," "Lifestyle Bowls," and "Sides," along with prices. There are navigation options like "Overview," "Locations," and "Menu," as well as a "Full menu" button at the bottom. The top includes the Google logo, search bar, and system status icons.

Current Action Thought:

The task requires opening a search for Music event in New York, but the current page is not related to it. I need to return to the main interface of the app first.

So the next Action is:

Click on home button in the upper left part of the screen ✓

PRESS the Back button ✓

Figure 6: An example from **AITZ** demonstrates that when the task and image are the same, multiple actions may navigate to the same page.

Potential correct space ratio. The proportion of $|\alpha| + |\beta|$ represents the potential correct space on the training data, and the change of this metric can clearly express the agent's ability to repair and reason out the correct process based on the correct answer.

G Computational Cost of IPL Across Iterations

As shown in Table 9, while the first IPL iteration incurs higher cost due to the larger volume of preference data, subsequent iterations are significantly lighter. The training time per round decreases rapidly, as the model generates fewer low-quality samples and requires fewer updates. In fact, by the third iteration, the training time becomes comparable to or even lower than the initial supervised fine-tuning (SFT) stage.

Therefore, the overall compute overhead of IPL remains moderate and manageable, especially considering its performance gains. Compared to SFT, IPL introduces only a modest increase in compute, but brings substantial improvements in reasoning and generalization.

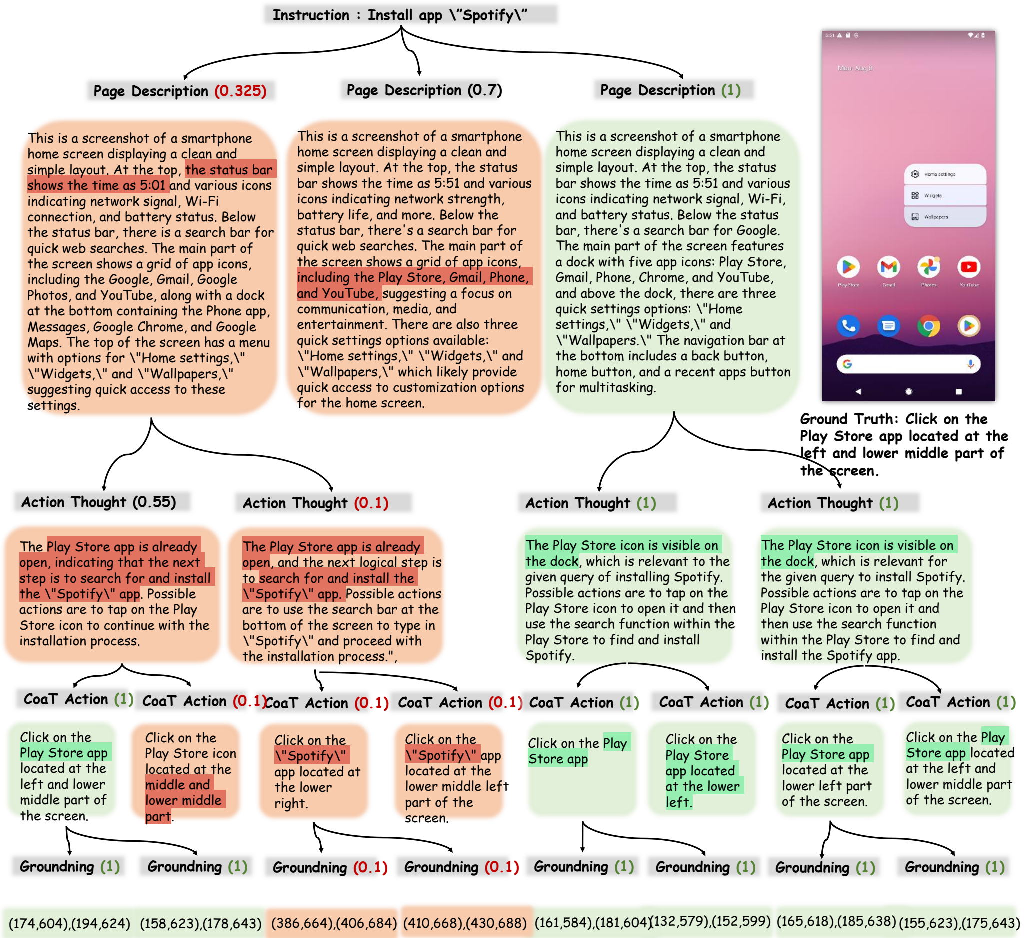

This is a screenshot of a smartphone home screen displaying a clean and simple layout. At the top, the status bar shows the time as 5:01 and various icons indicating network signal, Wi-Fi connection, and battery status. Below the status bar, there is a search bar for quick web searches. The main part of the screen shows a grid of app icons, including the Google, Gmail, Google Photos, and YouTube, along with a dock at the bottom containing the Phone app, Messages, Google Chrome, and Google Maps. The top of the screen has a menu with options for \"Home settings,\" \"Widgets,\" and \"Wallpapers,\" suggesting quick access to these settings.

This is a screenshot of a smartphone home screen displaying a clean and simple layout. At the top, the status bar shows the time as 5:51 and various icons indicating network strength, battery life, and more. Below the status bar, there's a search bar for quick web searches. The main part of the screen shows a grid of app icons, including the Play Store, Gmail, Phone, and YouTube, suggesting a focus on communication, media, and entertainment. There are also three quick settings options available: \"Home settings,\" \"Widgets,\" and \"Wallpapers,\" which likely provide quick access to customization options for the home screen.

This is a screenshot of a smartphone home screen displaying a clean and simple layout. At the top, the status bar shows the time as 5:51 and various icons indicating network signal, Wi-Fi, and battery status. Below the status bar, there's a search bar for Google. The main part of the screen features a dock with five app icons: Play Store, Gmail, Phone, Chrome, and YouTube, and above the dock, there are three quick settings options: \"Home settings,\" \"Widgets,\" and \"Wallpapers.\" The navigation bar at the bottom includes a back button, home button, and a recent apps button for multitasking.

Ground Truth: Click on the Play Store app located at the left and lower middle part of the screen.

The Play Store app is already open, indicating that the next step is to search for and install the \"Spotify\" app. Possible actions are to tap on the Play Store icon to continue with the installation process.

The Play Store app is already open, and the next logical step is to search for and install the \"Spotify\" app. Possible actions are to use the search bar at the bottom of the screen to type in \"Spotify\" and proceed with the installation process.",

The Play Store icon is visible on the dock, which is relevant to the given query of installing Spotify. Possible actions are to tap on the Play Store icon to open it and then use the search function within the Play Store to find and install Spotify.

The Play Store icon is visible on the dock, which is relevant for the given query to install Spotify. Possible actions are to tap on the Play Store icon to open it and then use the search function within the Play Store to find and install the Spotify app.

Click on the Play Store app located at the left and lower middle part of the screen.

Click on the Play Store icon located at the middle and lower middle part.

Click on the \"Spotify\" app located at the lower right.

Click on the \"Spotify\" app located at the lower middle left part of the screen.

Click on the Play Store app

Click on the Play Store app located at the lower left.

Click on the Play Store app located at the lower left part of the screen.

Click on the Play Store app located at the left and lower middle part of the screen.

Figure 7: A sampling tree from **AITZ** demonstrates how the value is calculated.

H Case Study

Unstable annotation preferences. As shown in Figure 5, the left section illustrates two different annotation preferences when searching for an app from the Home Page: **SCROLL UP** and **SCROLL LEFT**, leading to different destination pages. The right part shows the overall preference distribution when annotators need to find an app. In rare cases, the annotation involves clicking on Google Play Store to perform a search. This phenomenon is quite common because, fundamentally, the task completion paths for a UI Agent are diverse. This is also the key difference between online evaluation and offline data evaluation. From this, we observe that RL training on data with unstable preferences performs worse than SFT (e.g., AITZ SCROLL). This is because the DPO pair training method inherently attempts to correct errors in sampled preferences. As a result, the agent oscillates between two decisions when encountering the same GUI and instruction, failing to achieve consistent alignment.

Action Equivalence. Unlike Unstable Annotation Preferences, where different actions lead to different but equivalent pages, the issue here arises from annotators' random labeling habits in the training data, preventing the model from learning a consistent preference. Action Equivalence refers to the phenomenon where multiple actions on the same page can lead to the target page. However, since only one action is annotated as correct, other valid actions are mistakenly treated as incorrect. As shown in Figure 6, after entering a search query, clicking on a suggested item in the recommendation bar, and pressing the Enter key on the keyboard produce the same effect. Similarly, when navigating back, clicking the on-screen back button and pressing the hardware back button yield the same outcome.

Thinking-Level Sampling. As shown in Figure 7, unlike mathematical reasoning, the CoaT process may not exhibit clear logical or computational errors. For a given action, a sampling CoaT data may produce hallucinations (Page Description) due to insufficient detail in the page description or fabricated elements; generate repetitive thoughts (Action Thought) due to neglecting action history; describe the wrong relative position of the correct element (CoaT Action); or misgrounding an element (Grounding), which is then classified as a negative sample. At the same time, outputs with more detailed and accurate descriptions, diversified thoughts, and different ways of describing the same widget are classified as positive samples. Negative examples may be disadvantageous compared to positive examples, for example, because the description of the page is not detailed enough or the positioning of the elements is not accurate enough. At the same time, the wrong process may also give the correct result, but this is a very rare case. In this example, negative samples are generated due to the following three reasons: (1) **Rough page description:** The page contains eight app icons, but the agent's description includes only four apps: Play Store, Gmail, Phone, and YouTube; (2) **Hallucinated Thought:** The agent is unclear about its current page location. In reality, it is on the Home page, but it mistakenly believes it is in the Play Store (e.g., ”The Play Store app is already open"). (3) **Fabricated Position and Elements:** The agent generates the action "Click on the ’Spotify’ app", even though there is no Spotify icon on the current page. This hallucination may stem from the instruction. Additionally, the Play Store icon should be located at the lower left part of the screen, but the agent incorrectly describes it as being in the middle and lower middle part.

I USAGE OF LLM STATEMENT

This paper utilized an LLM to improve the clarity and fluency of the text.